Topological triplon band and edge states in the spin dimer antiferromagnet $Ba_2CuSi_2O_6Cl_2$

Institute of Multidisciplinary Research for Advanced Materials
Tohoku University
Kazuhiro Nawa

The 2nd Asia pacific workshop on quantum magnetism
ICTS, 2018/12/04

K. Nawa et al., cond-mat arXiv:1810.08931 (2018).

Experimental team

Sample Preparation and Characterization

Tanaka Kimihiko, Kurita Nobuyuki, Hidekazu Tanaka
(Tokyo Inst. Tech.)

Inelastic neutron scattering experiments

Tanaka Kimihiko, Kurita Nobuyuki, Hidekazu Tanaka
(Tokyo Inst. Tech.)
Kazuhiro Nawa, Taku J Sato (Tohoku Univ.)
Seiko Kawamura, Kenji Nakajima (J-PARC)

Single crystal XRD diffraction experiments

Haruki Sugiyama, Hidehiro Uekusa
(Tokyo Inst. Tech.)

Thanks for discussion

Masashige Matsumoto (Sizuoka Univ.) and Kentaro Nomura (Tohoku Univ.)

Contents

- Introduction
  Topological properties on bosonic system
  a spin dimer antiferromagnet $Ba_2CuSi_2O_6Cl_2$

- Triplon bands of $Ba_2CuSi_2O_6Cl_2$
  investigated by inelastic neutron scattering experiments

- Topological character of triplon bands
  associated edge states

Topological bosonic bands

Magnons : Ferromagnet $Lu_2V_2O_7$

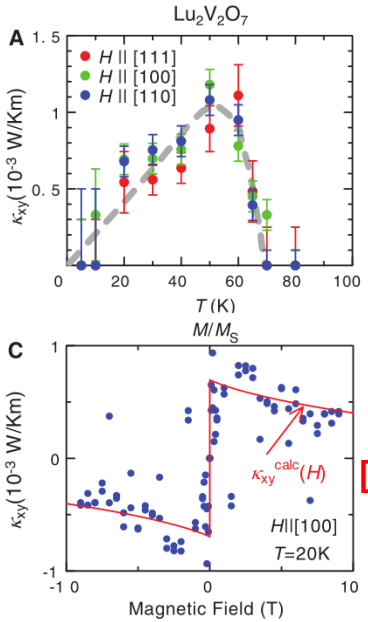

DM

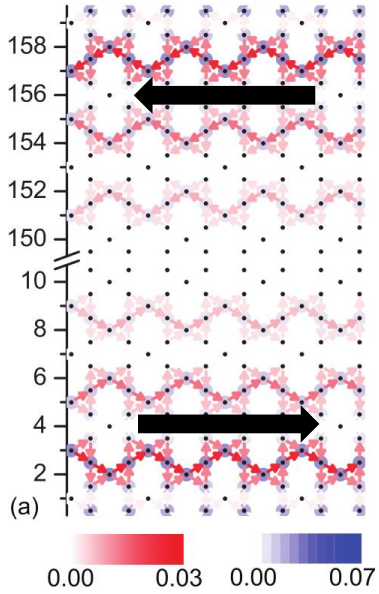

Y. Onose et al., Science **329**, 297 (2010).
L. Zhang et al., PRB **87**, 144101 (2013).

Thermal Hall effect : DM interactions produce non zero Berry curvature of excited bands

cf. Cu(1,3-bdc), Cu_3TeO_6

Necessary to reveal dispersion relations.

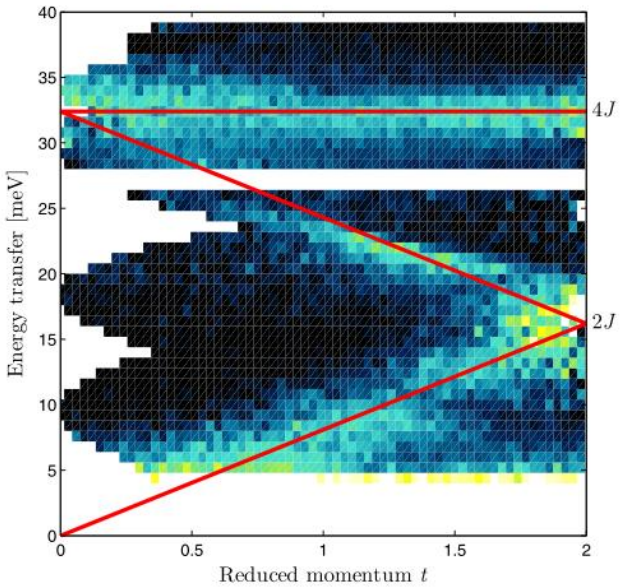

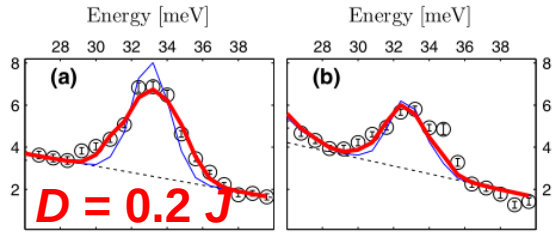

M. Mena et al., PRL **113**, 047202 (2014).
R. Chisnell et al., PRL **115**, 147201 (2015).
W. Yao et al. Nat. Phys. **14**, 1011 (2018).
S. Bao et al., Nat. Commun. **9**, 2591 (2018).

Magnetism of quantum dimer system

Magnons ← ordered magnets

Triplons ← a dimer antiferromagnet

ex. Isolated dimers with *S* = 1/2

intradimer interactions

$$H = NJ\boldsymbol{S}_1 \cdot \boldsymbol{S}_2$$

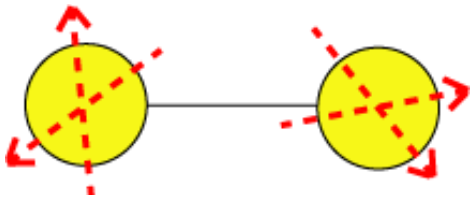

$$E_{\mathrm{T}} = \frac{1}{4}NJ : |S, S_z> = \left\{ \begin{array}{l} |1,1\rangle \\ |1,0\rangle \\ |1,-1\rangle \end{array} \right.$$

"Triplons"

$$E_{\mathrm{S}} = -\frac{3}{4}NJ : |S, S_z> = |0,0\rangle$$

Singlet ground state

In real compounds,

+ interdimer interactions

$$J'(S_i^+ S_j^- + S_i^- S_j^+)$$

hopping of triplons

Very simple but rich physics!

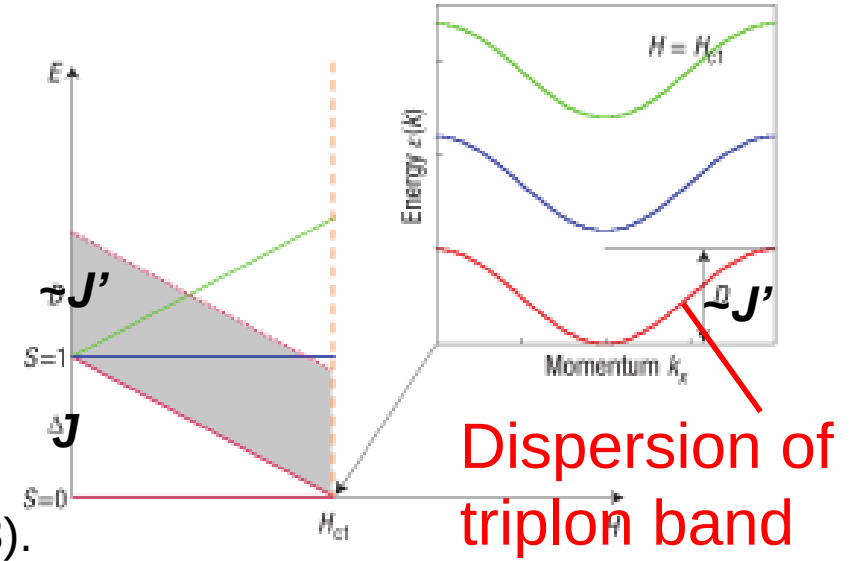

Dispersion of triplon band

T. Giamarchi *et al.*, Nature Physics, **4**, 198 (2008).

Topological triplon bands

Ex. $SrCu_2(BO_3)_2$

Shastry-Sutherland lattice

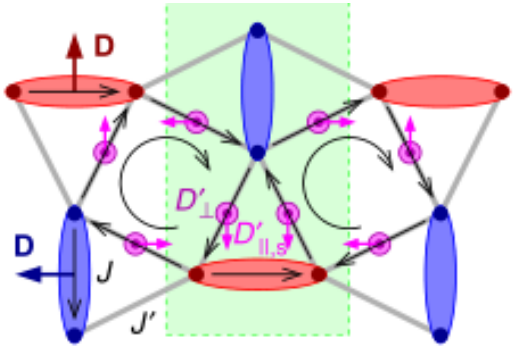

0 T < *H* < 1.4 T

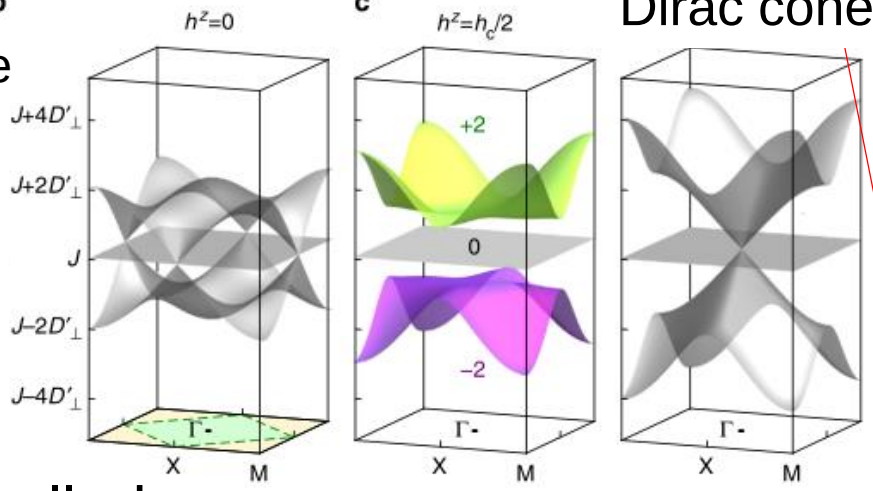

Spin-1 Dirac cone

H. Kageyama et al., PRL **84**, 5876 (2000).

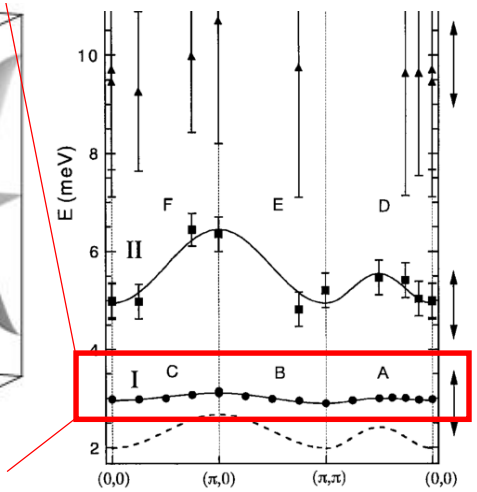

J' : hopping is cancelled

***D'* : complex hopping amplitudes**

➡ Triplon Hall effect

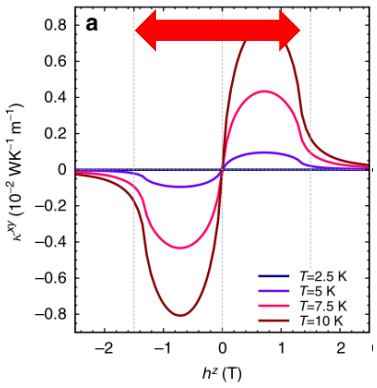

Thermally excited triplon edge states

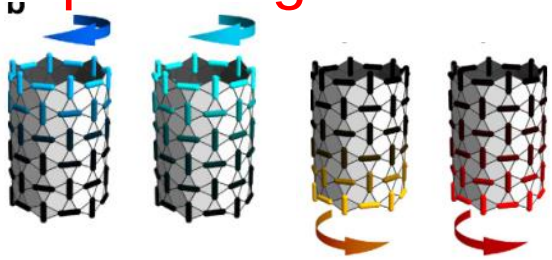

J. Romhanyi et al., Nat. Commun. **6**, 7805 (2015).

Nearly degenerate, dispersionless

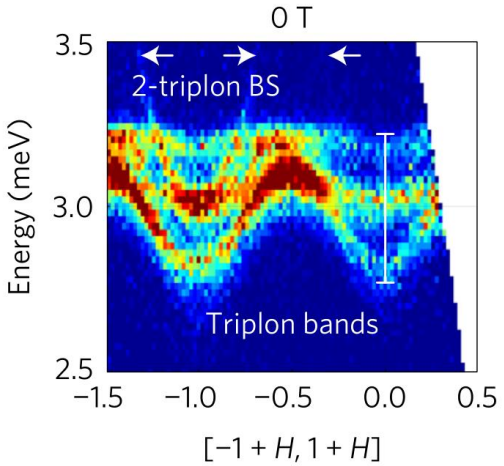

P. A. McMlarty et al., Nature Physics **13**, 736 (2017).

The dimer antiferromagnet $Ba_2CuSi_2O_6Cl_2$

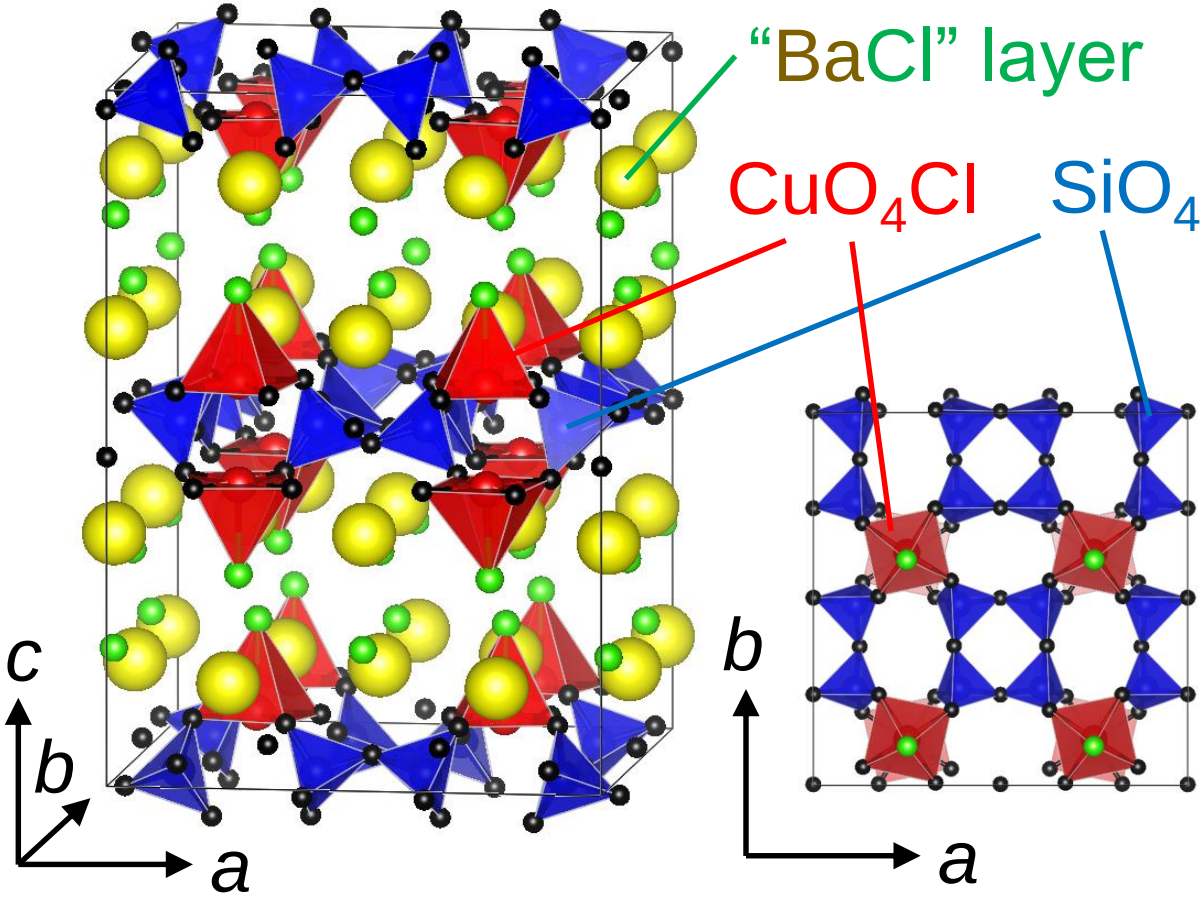

~

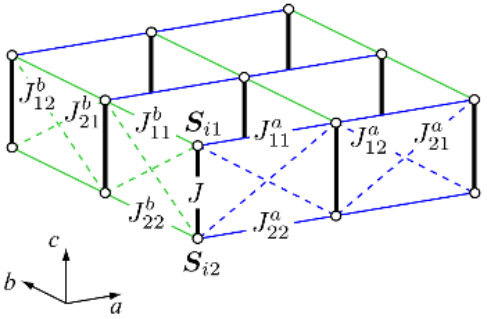

~~*Cmce*~~ → *Cmc*2_1
(loss of *a*-glide)
a = 13.8917(12) Å
b = 13.8563(11) Å
c = 19.6035(15) Å

Dimer forms a rectangular lattice

cf. E. C. Samulon et al., PRB **73**, 100407(R) (2006).

Structure is similar to that of $BaCuSi_2O_6$, but all dimers are equivalent and all layers are also equivalent.

M. Okada et al., Phys. Rev. B, **94**, 094421 (2016).

Magnetic properties of $Ba_2CuSi_2O_6Cl_2$

Consistent with χ and C of the spin dimer system.

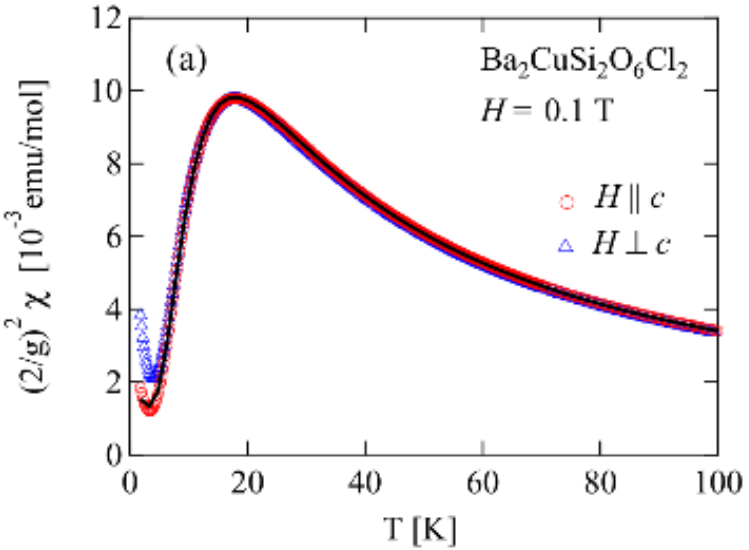

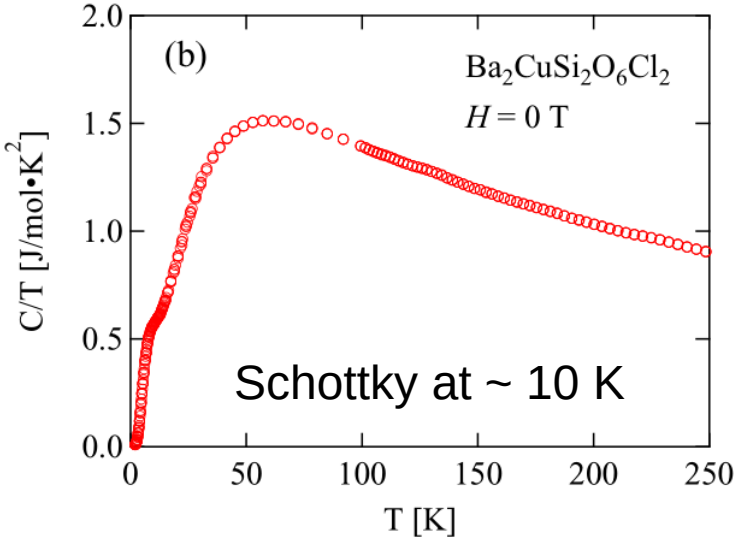

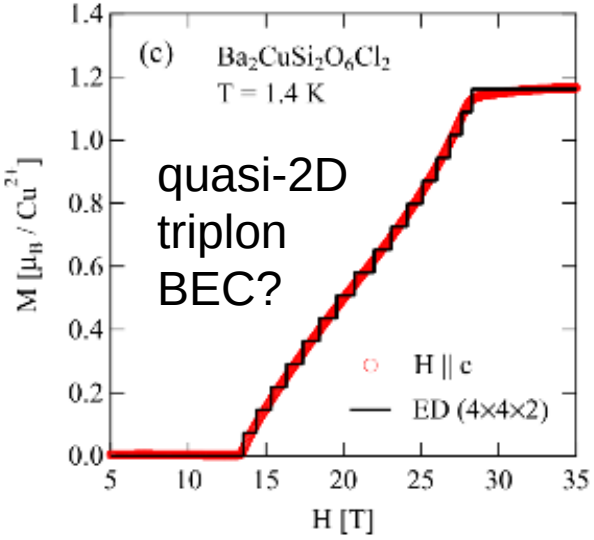

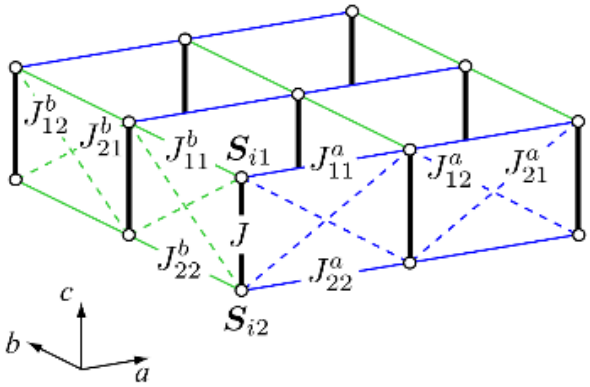

Intradimer

J = 2.42 meV

Interdimer

$J_{//}$ = 0.03 meV

$J_\times$ = 0.34 meV

Interlayer interaction : weak

M. Okada et al., Phys. Rev. B, **94**, 094421 (2016).

Triplon band splitting examined by inelastic neutron scattering experiments

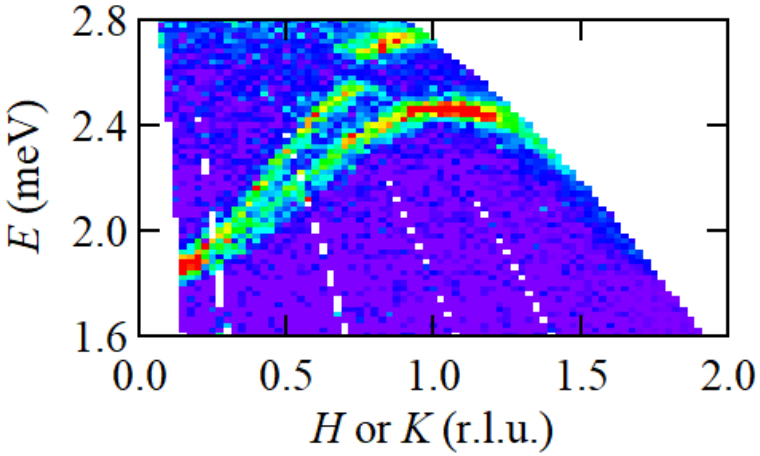

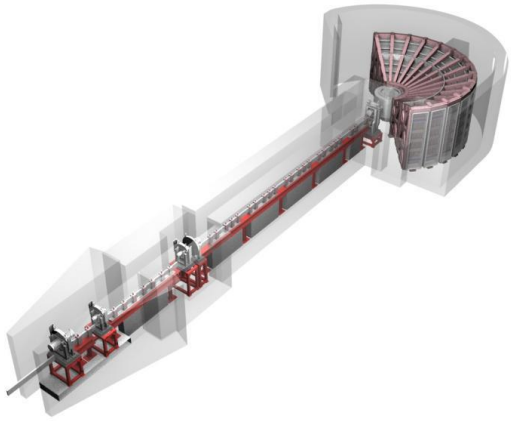

Cold-neutron disk chopper spectrometer AMATERAS (BL-14)

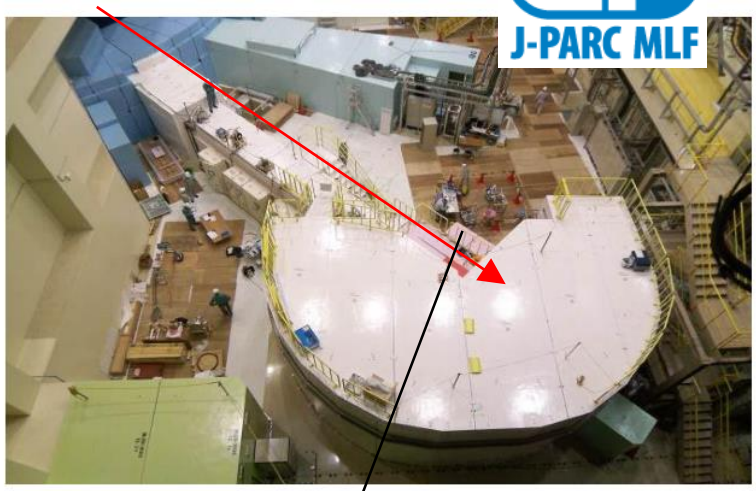

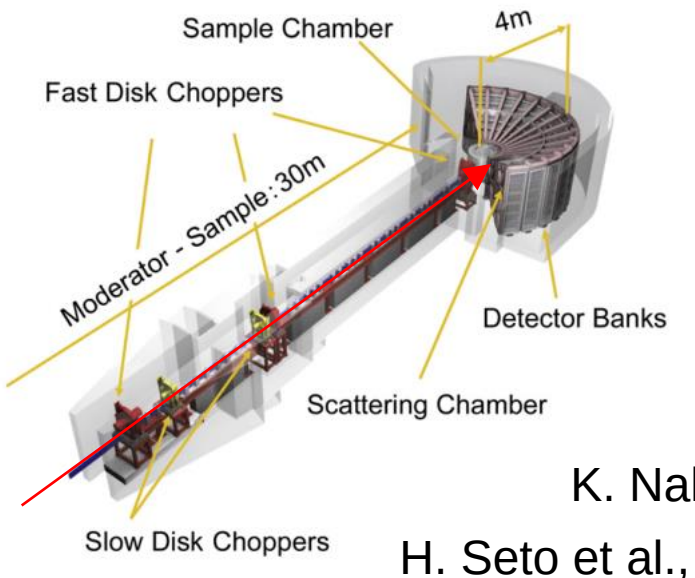

- Best performance for
  E_i = 1~20 meV
- High resolution ($\Delta E/E$ > 1 %) achieved by disk coppers
- A rate repetition multiplication

M. Nakamura et al., JPSJ **78**, 093002 (2009).

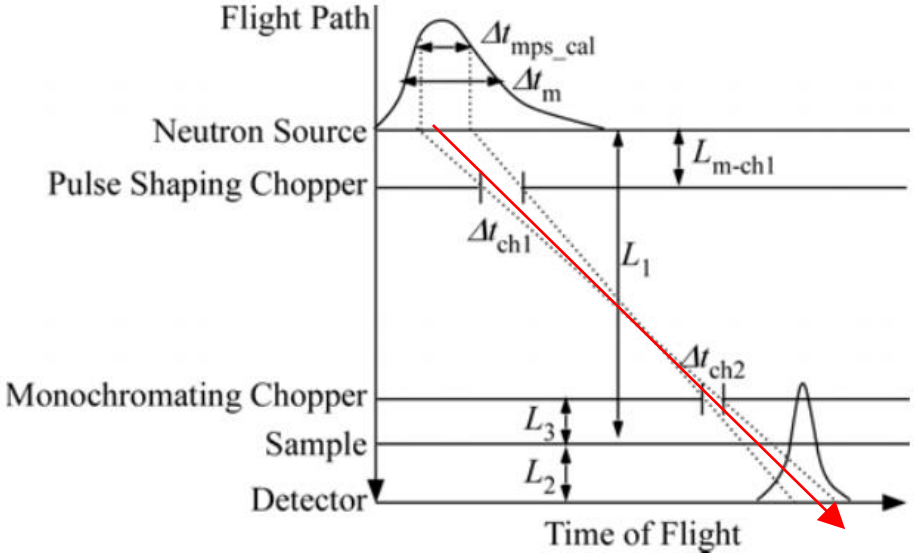

K. Nakajima et al., J. Phys. Soc. Jpn. 80, SB028 (2011).

H. Seto et al., Biochimica et Biophysica Acta **1861**, 3651 (2017).

Experiments

- Blue platelike single crystals were grown by a self-flux method
  (M. Okada et al., PRB **94**, 094421 (2016))
- Twenty pieces (~ 2 g) were coaligned on a rectangular Al plate (→).
- Few degrees of mozaicity.
- Main data measured with
  E_i = 5.92 meV ($\Delta E/E_i$ = 0.027)
  90 degree sample rotation around k_i // c*
- 0.3 K using ^{3}He refrigerator.
- Analyzed by the software suite UTSUSEMI.
  (Y. Inamura et al., JPSJ **82**, SA031 (2013).)

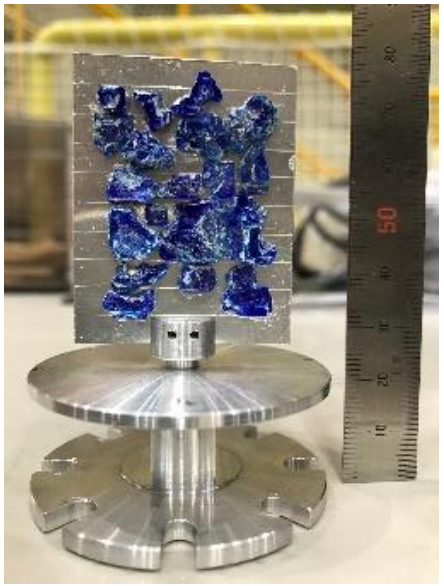

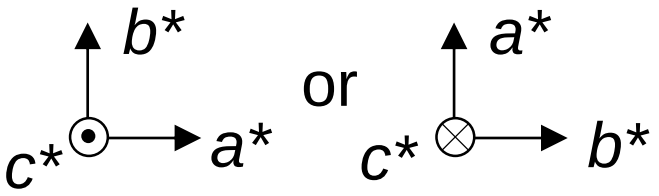

*a** and *b** cannot be distinguished because of crystallographic domains…

does not affect the analysis.
a axis length ~ *b* axis length

Split in triplon bands

Sliced along the 2D plane ($a^*(H)$ and $b^*(K)$)

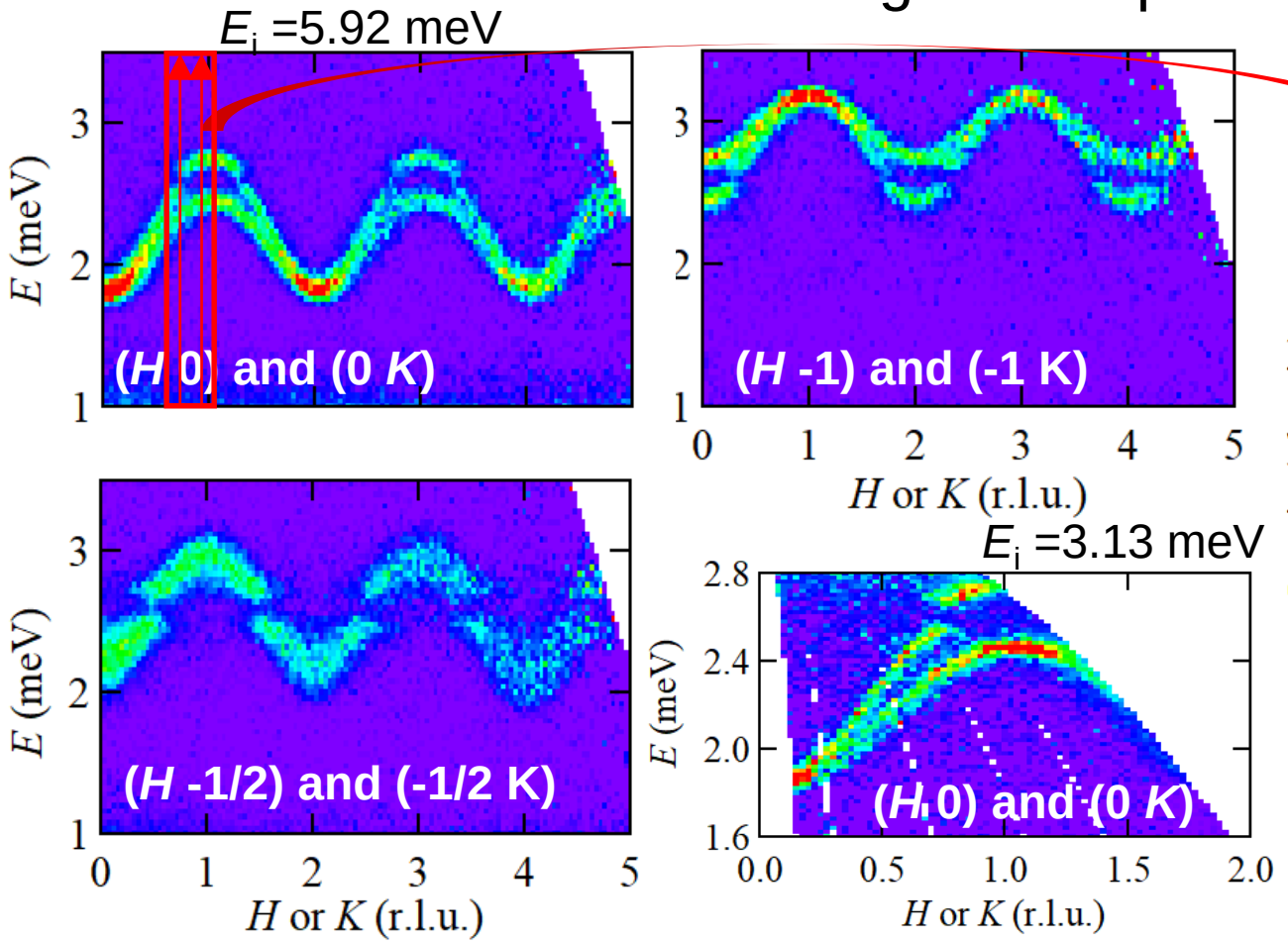

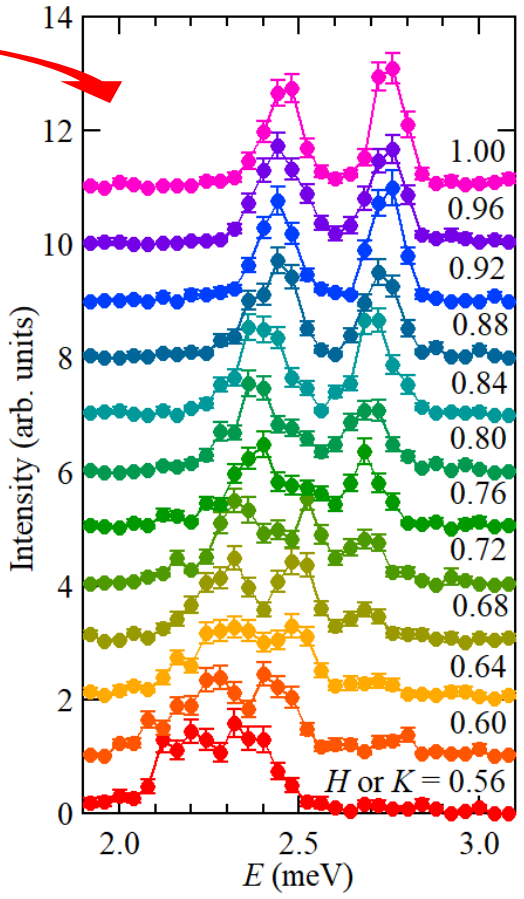

- Two dispersive branches at 2-3 meV : along *H* and *K*
- The minimum energy at even integers
- **Split of the band at 2.6 meV**

H or *K* = [H_0-0.1, H_0+0.1]
L = [-1.1, 8.0]

Dimer formation along *c*

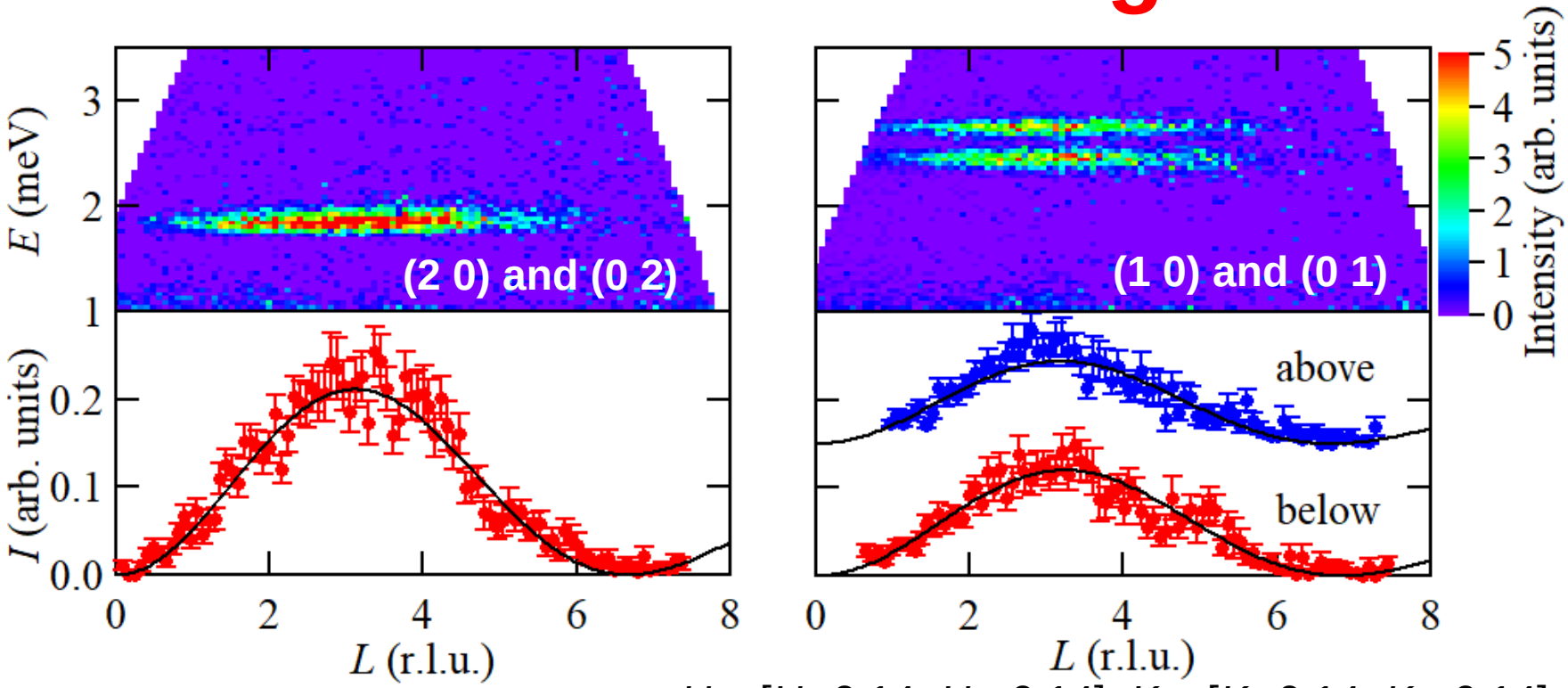

$H = [H_0\text{-}0.14, H_0\text{+}0.14]$, $K = [K_0\text{-}0.14, K_0\text{+}0.14]$

- Dispersionless along c^* (L) → negligible interlayer interactions

- Intensity oscillation → Dimer formation along *c*.

The fit yields 0.150(1)*c*
→ consistent with 0.148*c* (XRD).

$$I(Q,\omega) \sim |f(Q)|^2(1-\cos(\mathbf{Q}\cdot\mathbf{d}))$$

Form factor of Cu^{2+}

cf. Y. Sasago et al., Phys. Rev. B 55, 8357 (1997).

Why does the triplon band split?

A model as a starting point

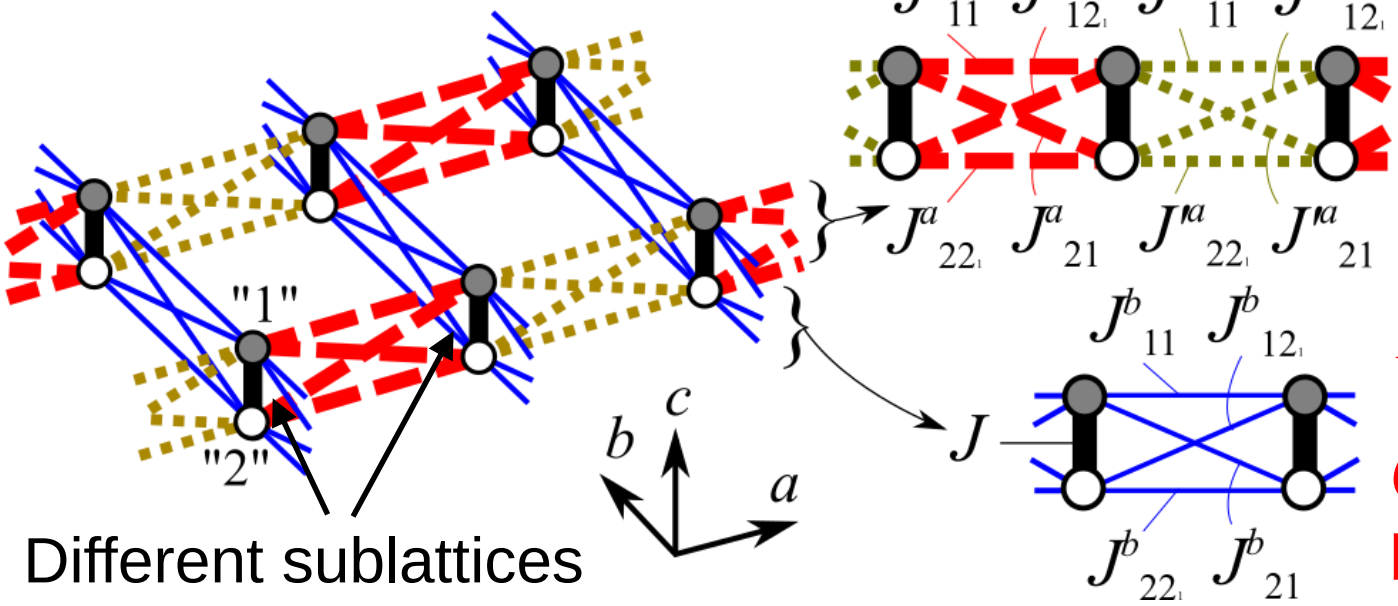

Different sublattices

2 (sublattice)
× 2 (*C* lattice)
× 2 (2_1 along *c*)
= 8 in a unit cell

Nearly rectangular

Cmc2_1: small bond alternation

$$\mathcal{H}_0 = J \sum_m \sum_n \boldsymbol{S}_{mn1} \cdot \boldsymbol{S}_{mn2}$$ **: Intradimer interactions**

$$\mathcal{H}' = \sum_{m+n=\text{even}} \sum_{\langle i,j \rangle} \left(J^a_{ij} \boldsymbol{S}_{mni} \cdot \boldsymbol{S}_{(m+1)nj} + J^{a\prime}_{ij} \boldsymbol{S}_{(m-1)ni} \cdot \boldsymbol{S}_{mnj} \right.$$

$$\left. + J^b_{ij} \boldsymbol{S}_{mni} \cdot \boldsymbol{S}_{m(n+1)j} + J^b_{ij} \boldsymbol{S}_{m(n-1)i} \cdot \boldsymbol{S}_{mnj} \right)$$

Interdimer interactions: 4 × 3 types

Effective Hamiltonian of triplons

Applying bond-operator approach

S. Sachdev and R. N. Bhatt, Phys. Rev. B **41**, 9323 (1990).

$$s^\dagger_{mn}|0\rangle = \frac{1}{\sqrt{2}}(|\uparrow\rangle_{mn1}|\downarrow\rangle_{mn2} - |\downarrow\rangle_{mn1}|\uparrow\rangle_{mn2})$$

$$t^\dagger_{xmn}|0\rangle = -\frac{1}{\sqrt{2}}(|\uparrow\rangle_{mn1}|\uparrow\rangle_{mn2} - |\downarrow\rangle_{mn1}|\downarrow\rangle_{mn2})$$

$$t^\dagger_{ymn}|0\rangle = \frac{i}{\sqrt{2}}(|\uparrow\rangle_{mn1}|\uparrow\rangle_{mn2} + |\downarrow\rangle_{mn1}|\downarrow\rangle_{mn2})$$

$$t^\dagger_{zmn}|0\rangle = \frac{1}{\sqrt{2}}(|\uparrow\rangle_{mn1}|\downarrow\rangle_{mn2} + |\downarrow\rangle_{mn1}|\uparrow\rangle_{mn2})$$

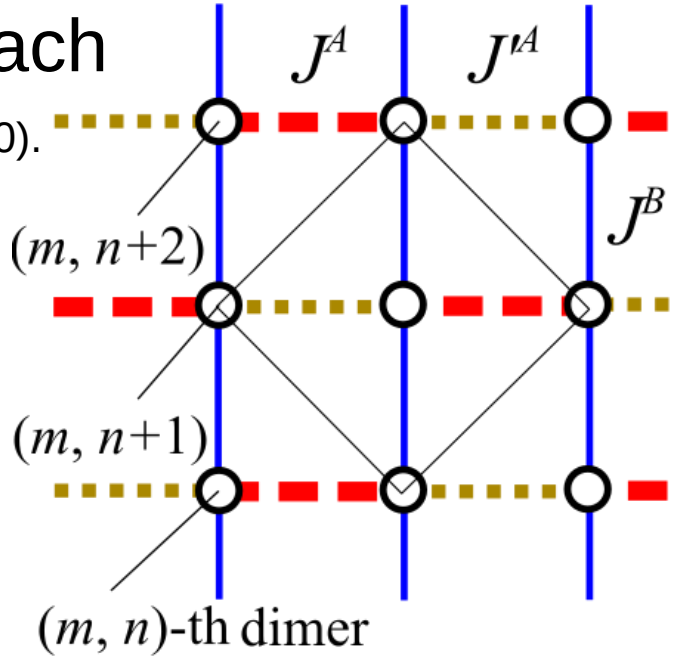

Projection to a triplon language

$$J^A = \tfrac{1}{4}(J^a_{11} + J^a_{22} - J^a_{12} - J^a_{21}), \cdots$$

Sublattice 1 or 2

$$\mathcal{H}_0 + \mathcal{H}' \sim \frac{1}{2}\sum_\alpha \sum_{\mathbf{k}} \left(t^{\dagger,1}_{\alpha\mathbf{k}}, t^{\dagger,2}_{\alpha\mathbf{k}}, t^1_{\alpha(-\mathbf{k})}, t^2_{\alpha(-\mathbf{k})}\right) \begin{pmatrix} J & \Lambda_{\mathbf{k}} & 0 & \Lambda_{\mathbf{k}} \\ \Lambda^*_{\mathbf{k}} & J & \Lambda^*_{\mathbf{k}} & 0 \\ 0 & \Lambda_{\mathbf{k}} & J & \Lambda_{\mathbf{k}} \\ \Lambda^*_{\mathbf{k}} & 0 & \Lambda^*_{\mathbf{k}} & J \end{pmatrix} \begin{pmatrix} t^1_{\alpha\mathbf{k}} \\ t^2_{\alpha\mathbf{k}} \\ t^{\dagger,1}_{\alpha(-\mathbf{k})} \\ t^{\dagger,2}_{\alpha(-\mathbf{k})} \end{pmatrix}$$

Mode : *x*, *y*, or *z* (**triply degenerate**)

$$\Lambda_{\mathbf{k}} = J^A e^{-ik_x a/2} + J^{A\prime} e^{ik_x a/2} + J^B\left(e^{-ik_y b/2} + e^{ik_y b/2}\right)$$

Dispersion relation obtained by diagonalizing $\sigma_3 M_k^{(4)}$ $\quad \sigma_3 = \mathrm{diag}(1, 1-1, -1)$

Absence of the gap in *Cmce*

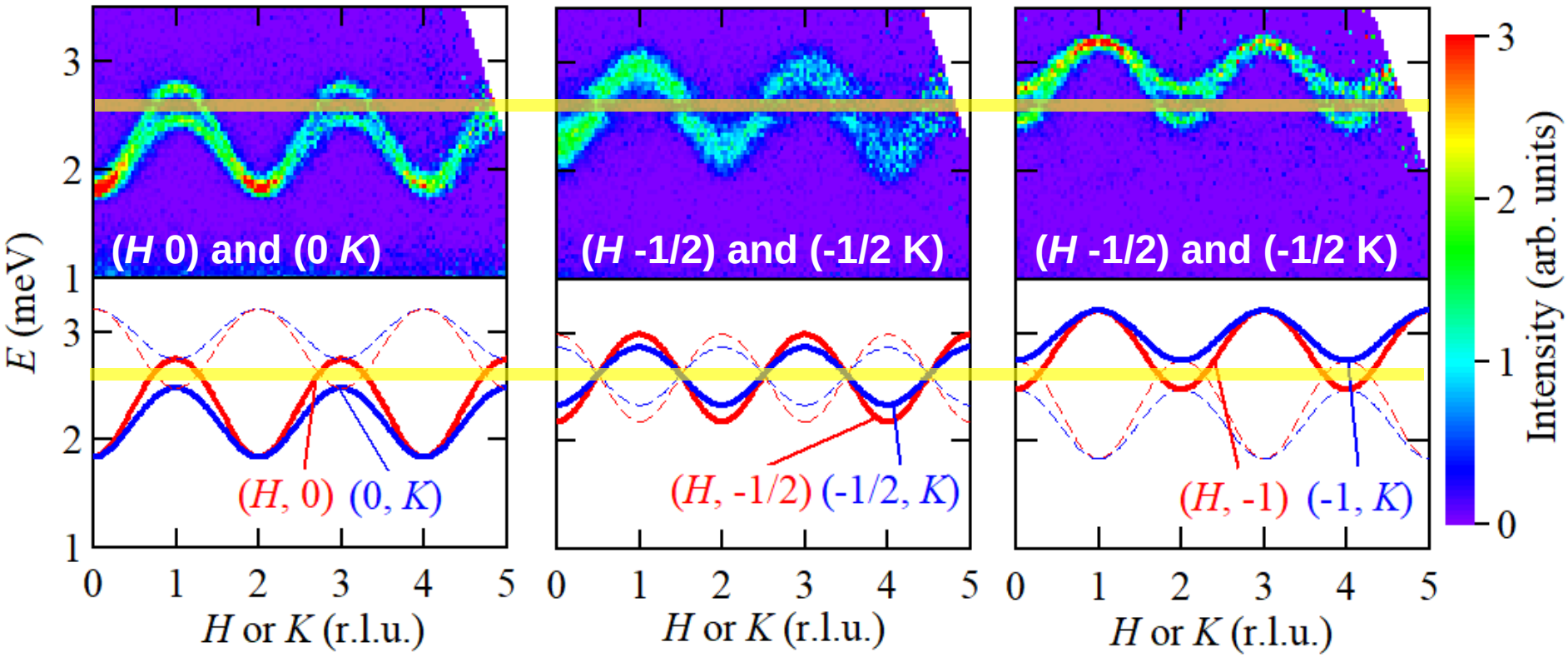

Two modes (solid/dashed)

H or *K* = [H_0-0.1, H_0+0.1], *L* = [-1.1, 8.0]

$$E_{\pm,\mathbf{k}} = \sqrt{J^2 \pm 2J|\Lambda_{\mathbf{k}}|} \quad J = 2.61, J^{\mathrm{A}} = J^{\mathrm{A}'} = -0.79, J^{B} = -0.53 \text{ (meV)}$$

Cmce $\rightarrow$ $J^{\mathrm{A}} = J^{\mathrm{A}'}$: Two sublattices become almost equivalent

The structure factor of one band is nearly zero.

Presence of the gap in $Cmc2_1$

(+ bond alternation)

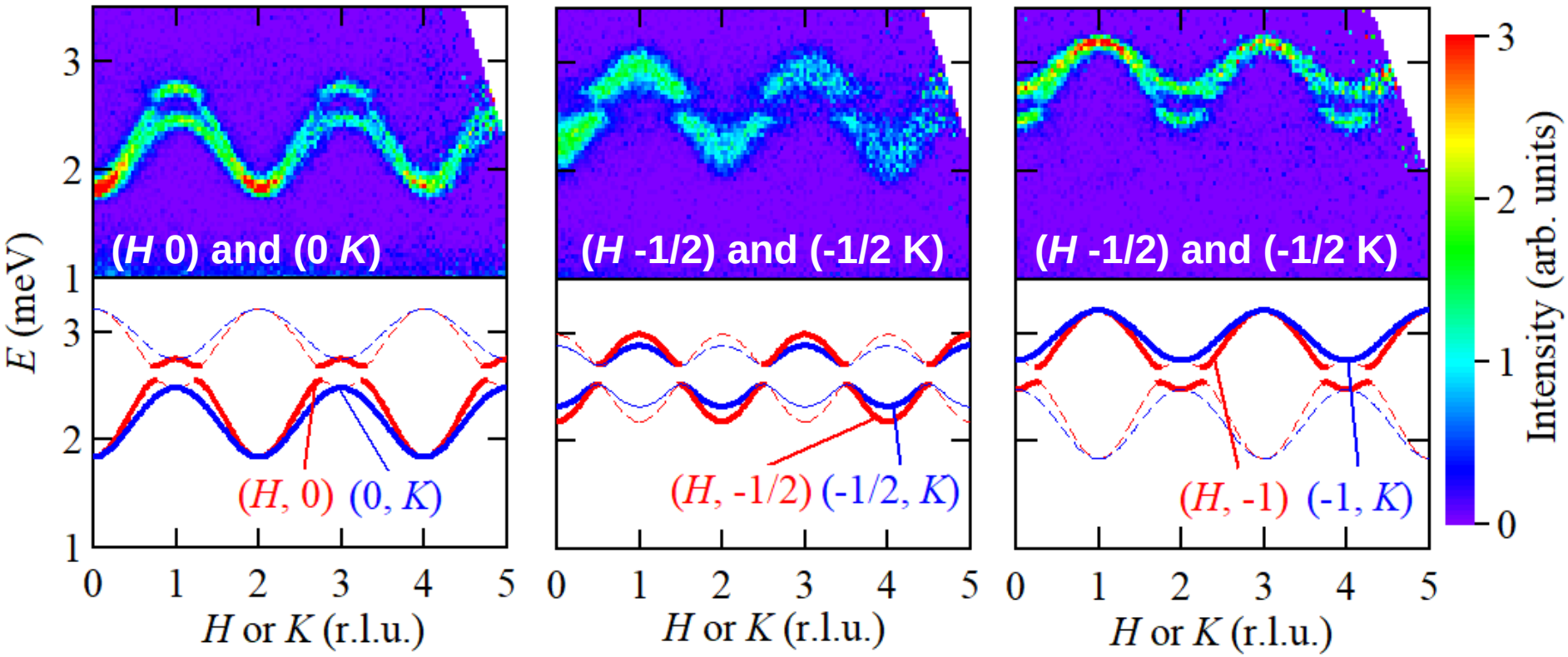

Two modes (solid/dashed)

H or K = [H_0-0.1, H_0+0.1], L = [-1.1, 8.0]

$$J = 2.61,\ J^{\mathrm{A}} = -0.97,\ J^{\mathrm{A}'} = -0.62,\ J^{B} = -0.53\ (\mathrm{meV})$$

reproduce the experiment results.

$Cmc2_1 \rightarrow$ possible to increase $|J^{\mathrm{A}}|$ and decrease $|J^{\mathrm{A}'}|$

Structure factor almost the same as those of the previous model.

Topologically protected triplon edge states

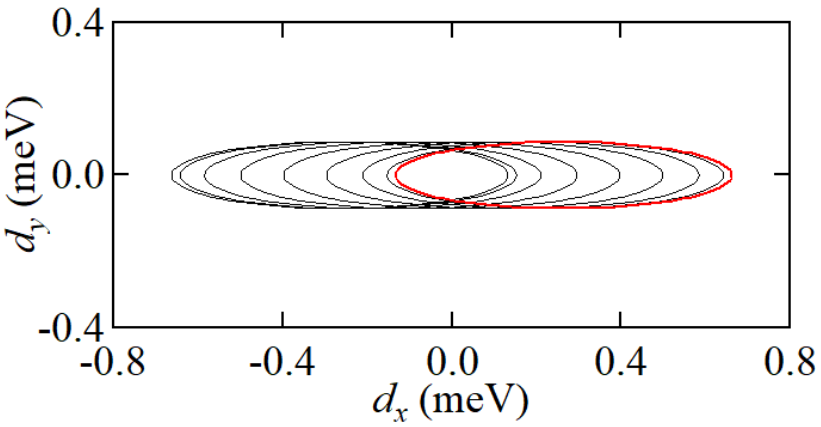

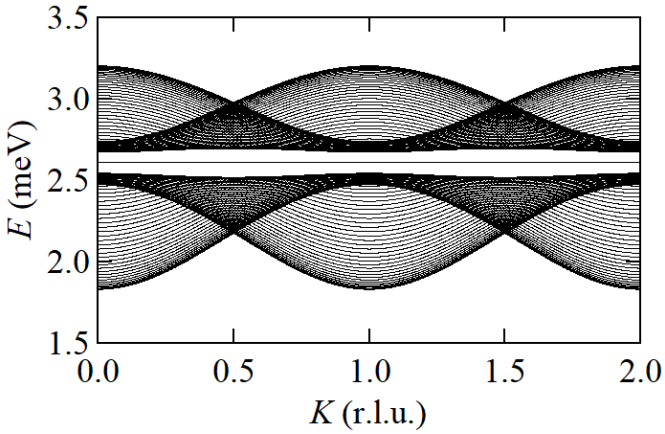

Band topology in $Ba_2CuSi_2O_6Cl_2$

$$\mathcal{H}_0+\mathcal{H}' \sim \frac{1}{2}\sum_{\alpha}\sum_{\mathbf{k}}\left(t^{\dagger,1}_{\alpha\mathbf{k}}, t^{\dagger,2}_{\alpha\mathbf{k}}, t^{1}_{\alpha(-\mathbf{k})}, t^{2}_{\alpha(-\mathbf{k})}\right)\underbrace{\begin{pmatrix} J & \Lambda_{\mathbf{k}} & 0 & \Lambda_{\mathbf{k}} \\ \Lambda^*_{\mathbf{k}} & J & \Lambda^*_{\mathbf{k}} & 0 \\ 0 & \Lambda_{\mathbf{k}} & J & \Lambda_{\mathbf{k}} \\ \Lambda^*_{\mathbf{k}} & 0 & \Lambda^*_{\mathbf{k}} & J \end{pmatrix}}_{\mathcal{M}^{(4)}_{\mathbf{k}}}\begin{pmatrix} t^{1}_{\alpha\mathbf{k}} \\ t^{2}_{\alpha\mathbf{k}} \\ t^{\dagger,1}_{\alpha(-\mathbf{k})} \\ t^{\dagger,2}_{\alpha(-\mathbf{k})} \end{pmatrix}$$

For simplicity, let's neglect pair-creation and pair-annihilation terms and think only a reduced matrix first…
(dispersion is not so much deformed by this procedure)

reduced into..

$$(\mathcal{H}_0+\mathcal{H}')_{\alpha} \sim \sum_{\mathbf{k}}\left(t^{\dagger,1}_{\mathbf{k}} t^{\dagger,2}_{\mathbf{k}}\right)\underbrace{\begin{pmatrix} J & \Lambda_{\mathbf{k}} \\ \Lambda^*_{\mathbf{k}} & J \end{pmatrix}}_{\mathcal{M}^{(2)}_{\mathbf{k}}}\begin{pmatrix} t^{1}_{\mathbf{k}} \\ t^{2}_{\mathbf{k}} \end{pmatrix}$$

Su-Schrieffer-Heeger (SSH) model

- Fermionic system : hopping of an electron on a chain
- **Two sublattice (A and B)**
- **Alternated hopping amplitude (v and w)**

(*cf.* polyacetylene)

W. Su *et al.*, Phys. Rev. Lett. **42**, 1698 (1979).

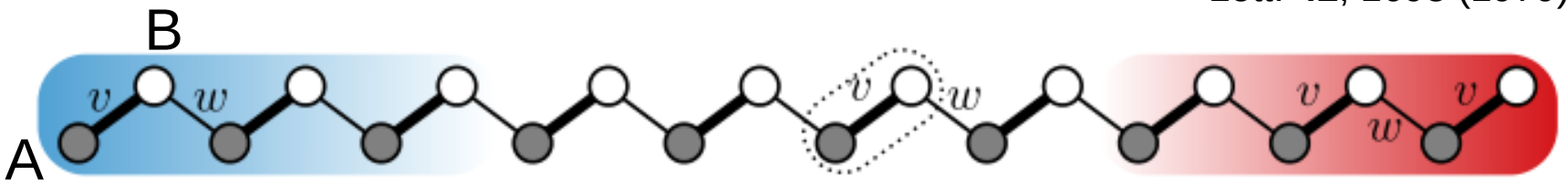

$$\mathcal{H}_{\mathrm{SSH}} \equiv \begin{pmatrix} 0 & v + we^{-ik} \\ v + we^{ik} & 0 \end{pmatrix} = \boldsymbol{d}(\mathbf{k}) \cdot \boldsymbol{\sigma}$$

$$\boldsymbol{d}(\mathbf{k}) = (\mathrm{Re}\Lambda_{\mathbf{k}}, -\mathrm{Im}\Lambda_{\mathbf{k}}, 0)\,, \Lambda_{\mathbf{k}} = v + we^{-ik}$$

: pseudomagnetic field

$$\boldsymbol{\sigma} = \left[\begin{pmatrix} 0 & 1 \\ 1 & 0 \end{pmatrix}, \begin{pmatrix} 0 & -i \\ i & 0 \end{pmatrix}, \begin{pmatrix} 1 & 0 \\ 0 & -1 \end{pmatrix} \right]$$

: pseudospin 1/2 (Pauli matrix)

$E = \pm|\boldsymbol{d}(\mathbf{k})| = \pm|\Lambda_{\mathbf{k}}|$: Two bands with an energy gap

Energy gap $\Delta = 2\mathrm{min}_{\mathbf{k}}\Lambda_{\mathbf{k}} = 2(|v| - |w|)$

J. K. Asbóth *et al.*, Lecture Notes in Physics, **919** (2016).

Relation between d_x and d_y in SSH

$$\boldsymbol{d}(\mathbf{k}) = (\mathrm{Re}\Lambda_{\mathbf{k}}, -\mathrm{Im}\Lambda_{\mathbf{k}}, 0)\,, \Lambda_{\mathbf{k}} = v + we^{-ik}$$

A single circle in a d_x-d_y plane

$w = 0$ $\quad$ $w = v$ $\quad$ $w >> v$

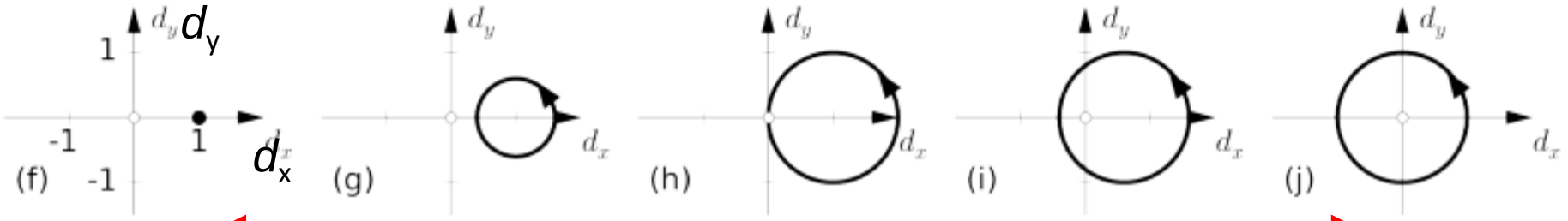

Winding number: 0 (gapped) | 0 (gapped) | gapless | 1 (gapped) | 1 (gapped)

$|w| < |v|$

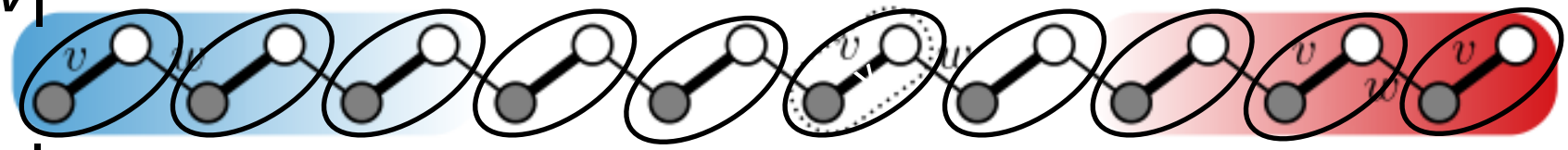

$|w| > |v|$

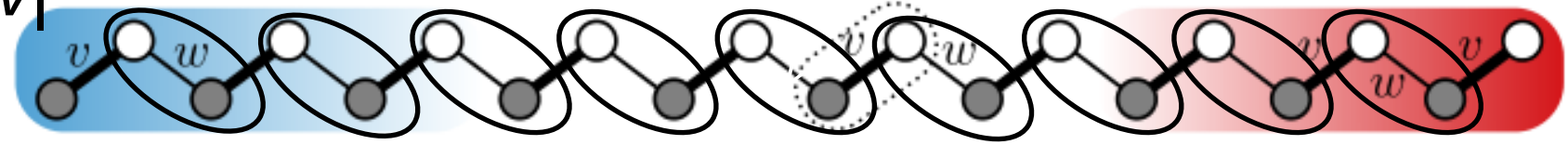

d_z(k) = 0 : cannot change winding number without closing the gap

topologically protected (by chiral symmetry)

Coupled SSH model

SSH chains coupled with an opposite alternating sequence

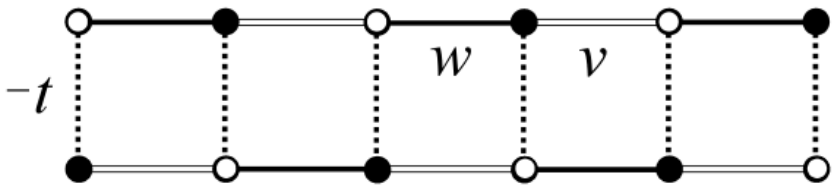

$$\boldsymbol{d}(\mathbf{k}) = (\mathrm{Re}\Lambda_{\mathbf{k}}, -\mathrm{Im}\Lambda_{\mathbf{k}}, 0)\,,$$
$$\Lambda_{\mathbf{k}} = we^{ik} + ve^{-ik} + t$$

C. Li *et al.*, Phys. Rev. B **96**, 125418 (2017).

A single ellipsis in a d_x-d_y plane

Two nontirvial gapped phases, separated by gapless phase

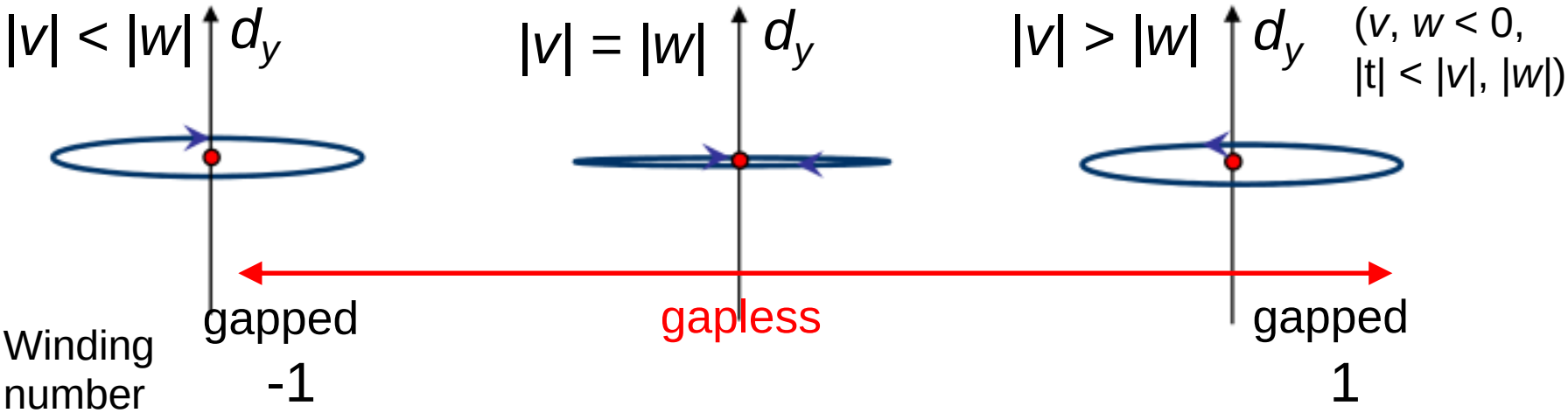

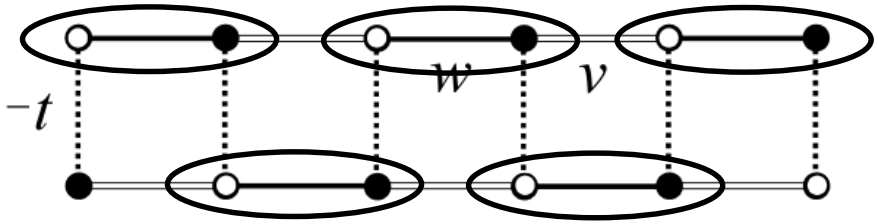

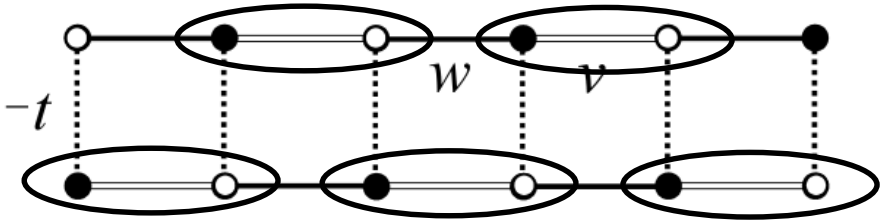

$Ba_2CuSi_2O_6Cl_2$ as a coupled SSH model

$$\mathcal{H}_d \equiv \begin{pmatrix} J & \Lambda_{\mathbf{k}} \\ \Lambda_{\mathbf{k}}^* & J \end{pmatrix} = J\mathbf{1} + \boldsymbol{d}(\mathbf{k}) \cdot \boldsymbol{\sigma}$$

shift energy
Edge modes
appear at J

$$\boldsymbol{d}(\mathbf{k}) = (\mathrm{Re}\Lambda_{\mathbf{k}}, -\mathrm{Im}\Lambda_{\mathbf{k}}, 0)$$

$$\Lambda_{\mathbf{k}} = J^A e^{-ik_x a/2} + J^{A\prime} e^{ik_x a/2} + J^B \left(e^{-ik_y b/2} + e^{ik_y b/2}\right)$$

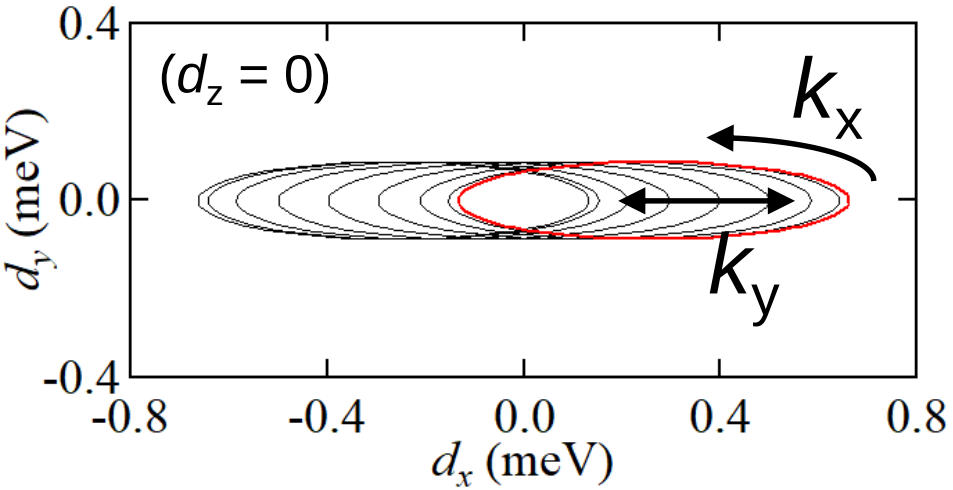

- k_x varied : a ellipsis.
- k_y varied : shift along d_x.

d : "aggregate" of ellipses

Fixing k_y

single ellipsis

The winding number is the same for the all k_y owing to $|J^B| < |J^A + J^{A'}|/2$. → quasi-1D extension of SSH

Coupled SSH model with fixed k_y

$|J^A| < |J^{A'}|$ $|J^A| = |J^{A'}|$ $|J^A| > |J^{A'}|$

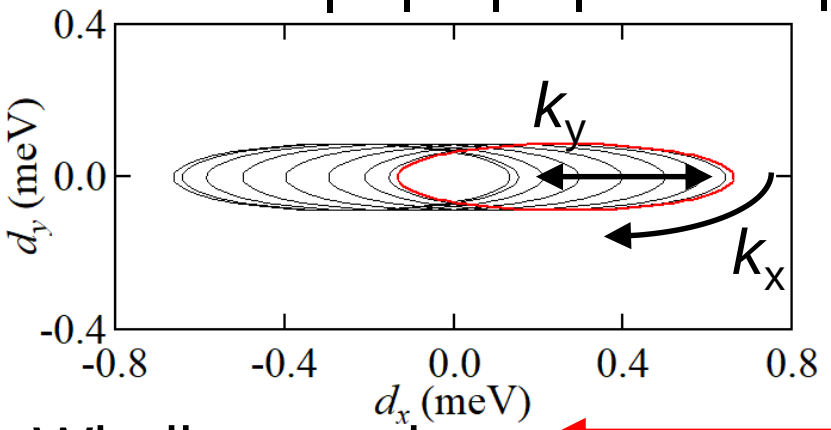

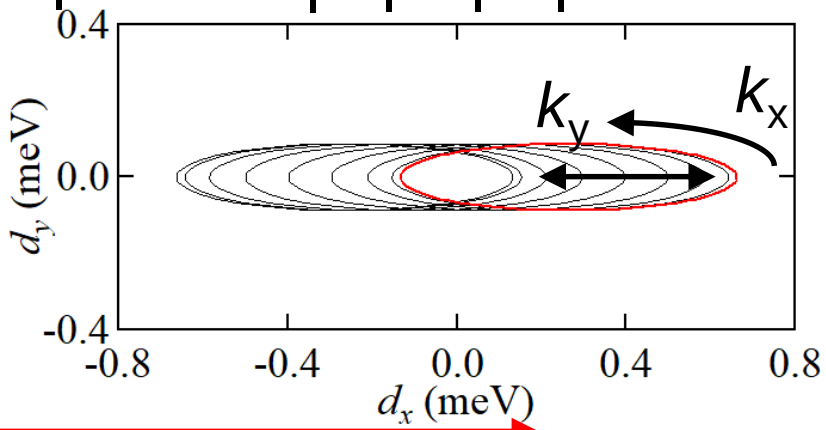

Winding number

-1 gapless 1

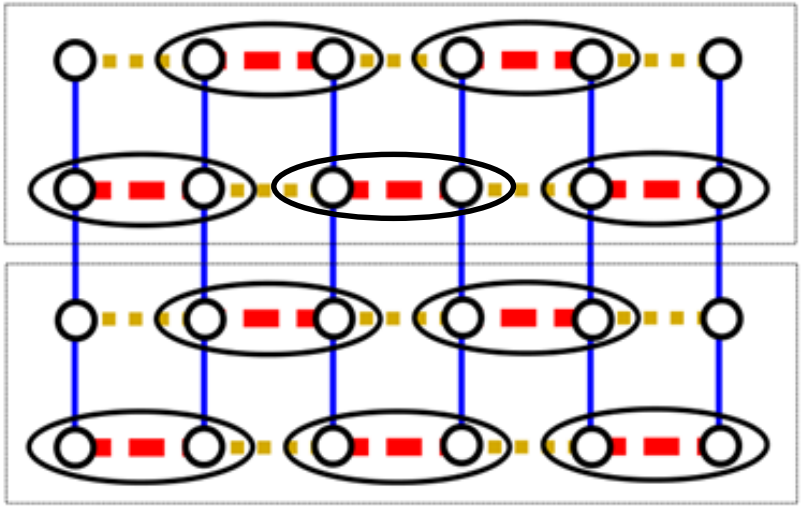

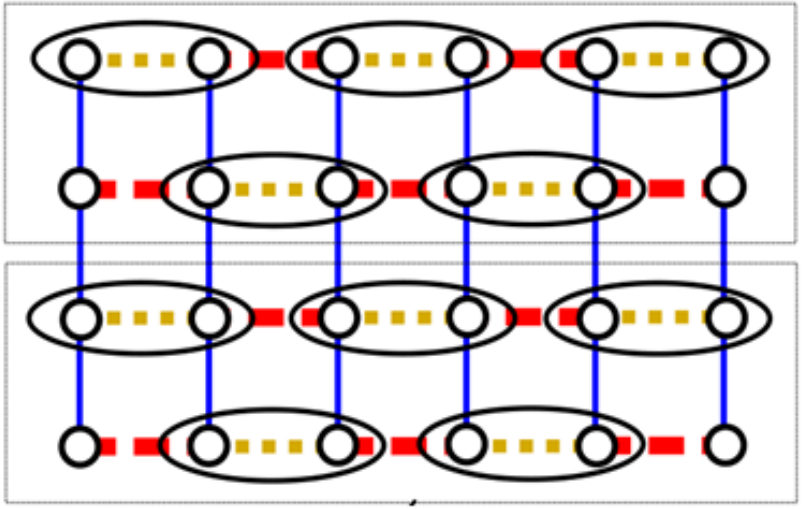

Alternation of J_A, J_A' → two sublattices → nontrivial topology

$d_z(k) = 0$ → topologically protected edge states (thermally excited)

Energy spectrum

Along *a*: Open boundary vs Periodic boundary

$$\mathcal{H}_{\mathrm{BdG}} = \begin{pmatrix} J\mathbf{1} + \mathbf{X_q} & \mathbf{X_q} \\ \mathbf{X_q} & J\mathbf{1} + \mathbf{X_q} \end{pmatrix}$$

$4N_a \times 4N_a$ matrix

$t^{\dagger,1}{}_{1ky}$, $t^{\dagger,2}{}_{1ky}$, …, $t^{\dagger,1}{}_{Naky}$, $t^{\dagger,2}{}_{Naky}$ "Anomalous term"

$J_q = 2J^B \cos(k_y b/2)$

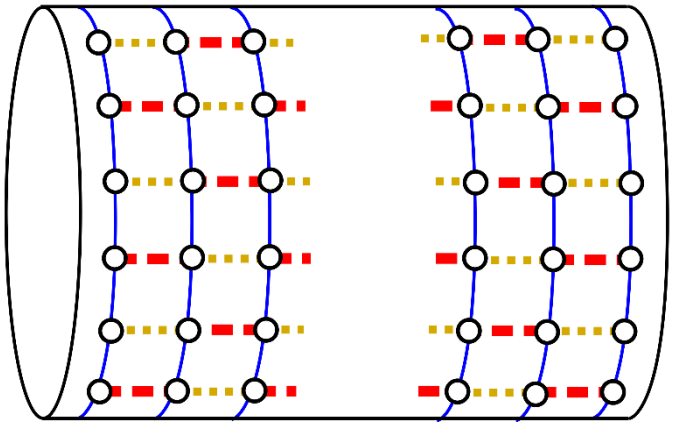

FT only along the *b* (not along the *a*)

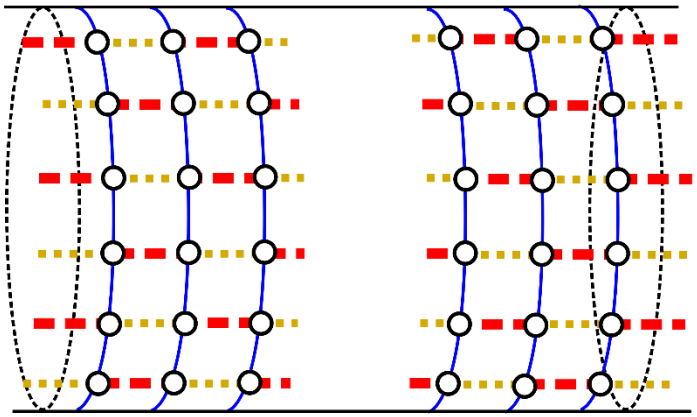

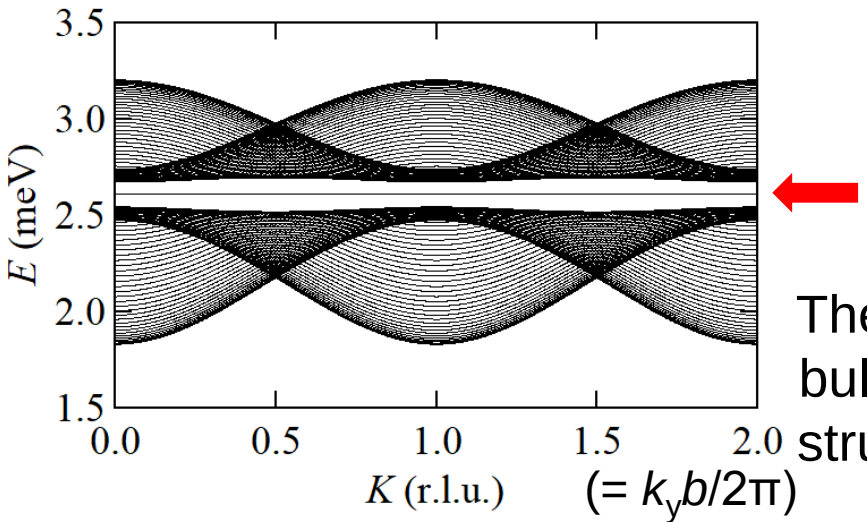

The same bulk band structures (= $k_y b/2\pi$)

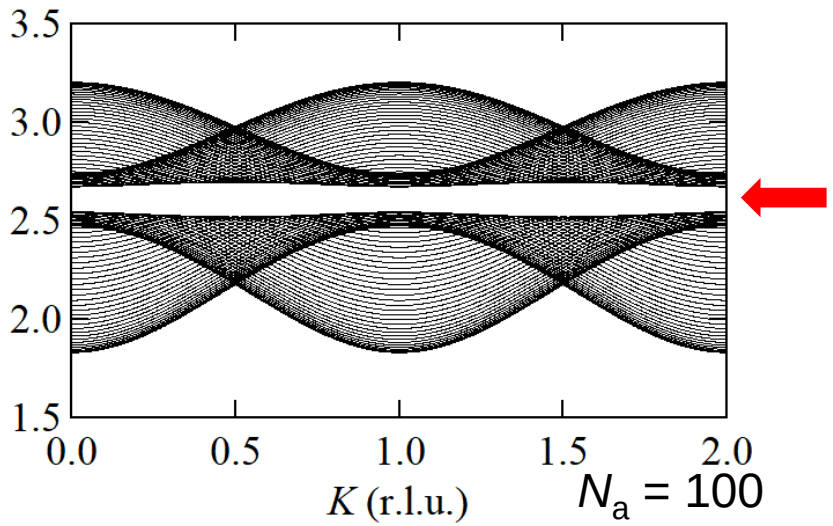

$N_a = 100$

Summary

- Spin excitation spectrum of $Ba_2CuSi_2O_6Cl_2$ exhibits two triplon bands with a small gap between them, which is due to the alternation of interdimer interactions.

- The triplon band topology is the same as the coupled SSH model, indicating the presence of topologically protected edge states.

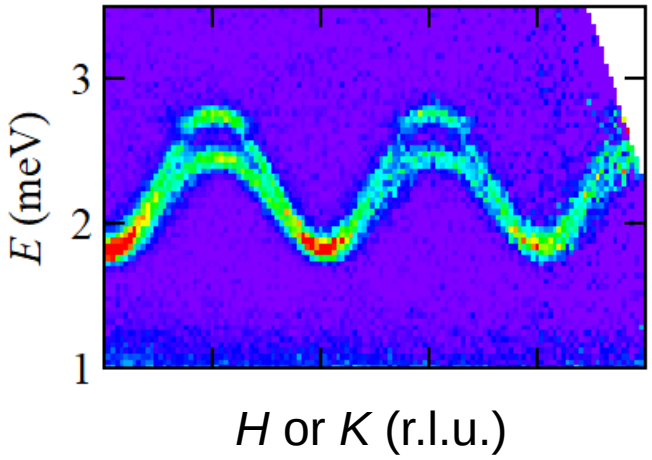

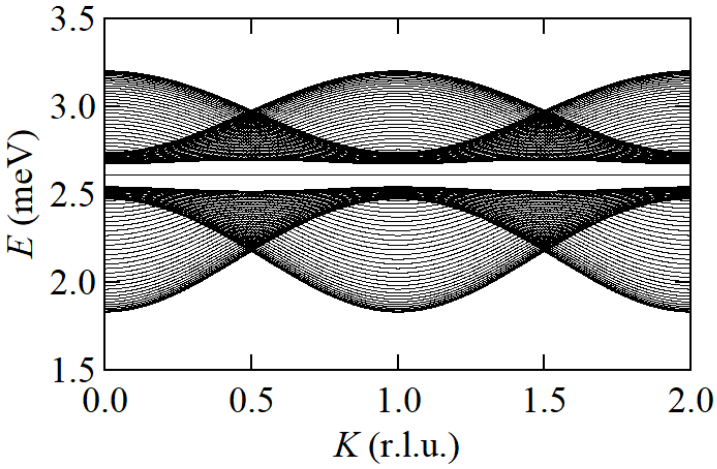

A large degeneracy near the ground states in “pyrochlore” antiferromagnet

$Na_3Mn(CO_3)_2Cl$

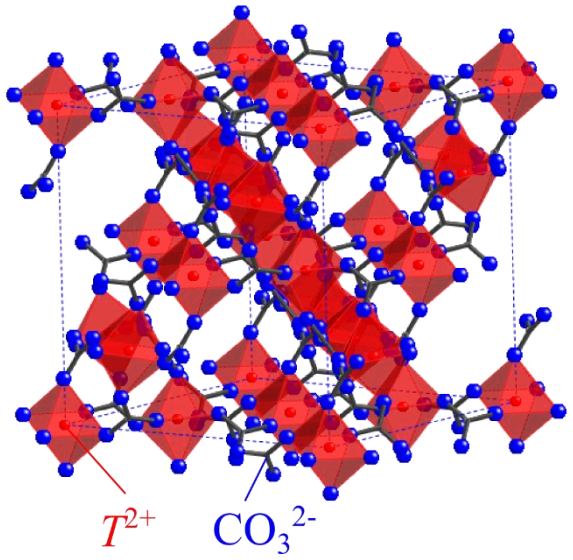

Although a short range order develops below θ_W = 40 K, the signature of a long range order is not found at 0.05 K (by NPD).

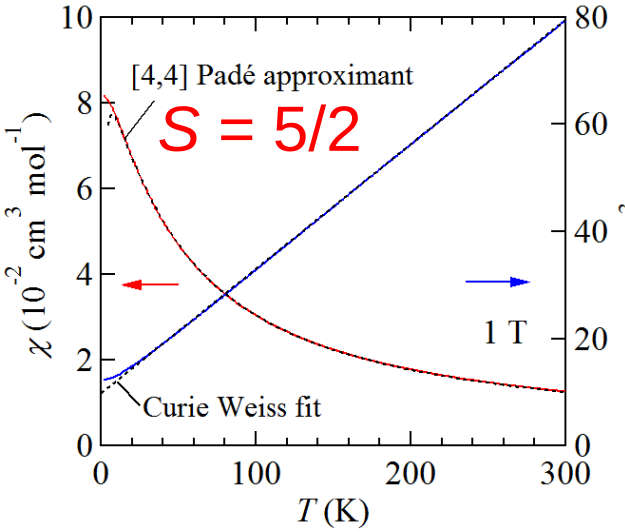

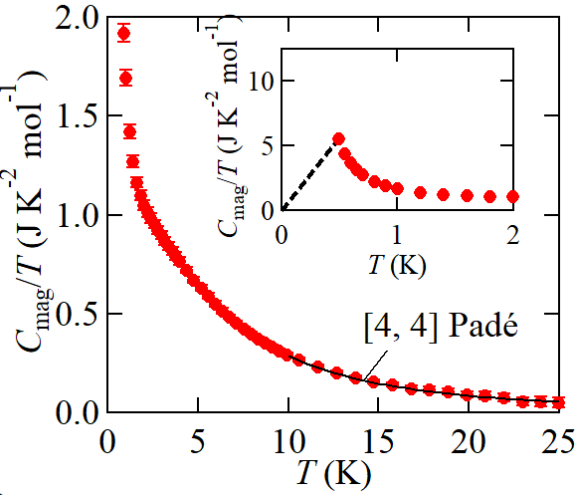

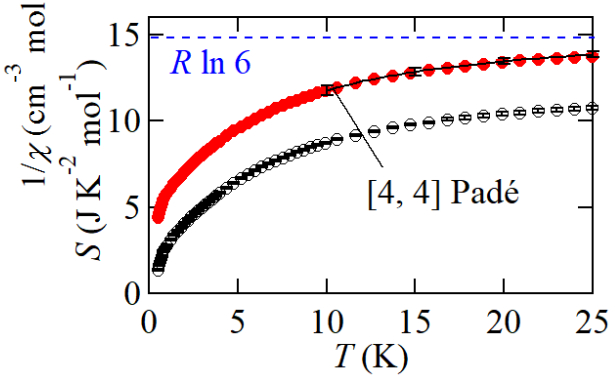

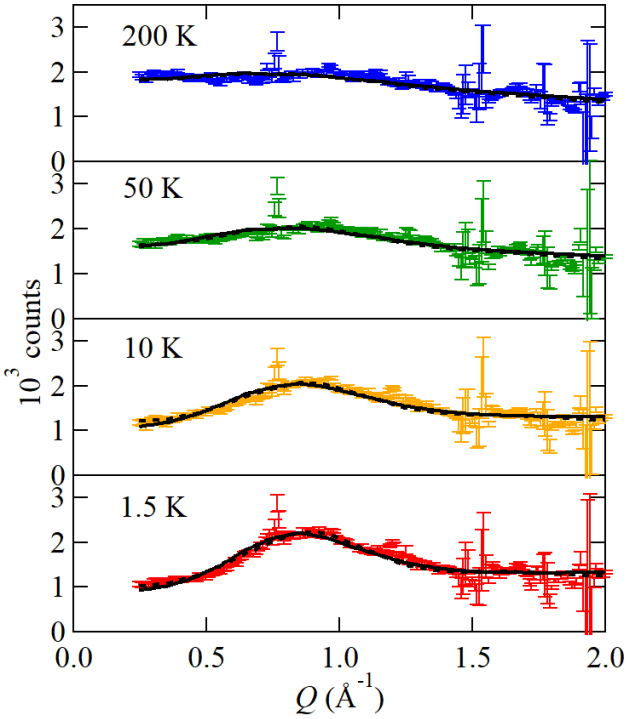

K. Nawa et al., Phys. Rev. B **98**, 144426 (2018).